AN ABSTRACT OF THE THESIS OF

Richard William Couch for the M. S. in Meteorology
(Name) (Degree)

Date thesis is presented May 15, 1963

Title SURFACE OBSERVATIONS OF THE ELECTRICAL CHARGES RETAINED BY PRECIPITATION

Redacted for Privacy

Abstract approved ______
(Major professor)

After comparing theories of precipitation electrification, this paper presents the design of a precipitation charge electrometer and a point discharge current meter. Data from these instruments make possible a statistical comparison of cloud heights and electrical charge on precipitation. A 50-minute period of comparison shows a 37 percent dependency of precipitation charge on cloud heights. Analysis of five independent samples of charge magnitude and drop size show a 45 percent interdependency. Major limiting factors include modifications of the drop charge during descent and sampling of the drop size distribution at a remote location from the precipitation charge measurement. Further research should include a method of measuring the variations in precipitation charge during descent and samples during many weather situations.

SURFACE OBSERVATIONS OF THE ELECTRICAL CHARGES RETAINED BY PRECIPITATION

by

RICHARD WILLIAM COUCH

A THESIS

submitted to

OREGON STATE UNIVERSITY

in partial fulfillment of
the requirements for the
degree of

MASTER OF SCIENCE

June, 1963

APPROVED:

Redacted for Privacy

Associate Professor of Physics

In Charge of Major

Redacted for Privacy

Chairman of Department of Physics

Redacted for Privacy

Dean of Graduate School

Date thesis is presented May 15, 1963

Typed by Jolene Hunter Wuest

ACKNOWLEDGEMENT

The nature of the work presented in this thesis depends of necessity on the efforts of many able and dedicated research participants. In cognizance, the author wishes to sincerely thank Dr. Fred W. Decker whose vision and forethought provided the opportunity and facilities for this research; John D. Pembrook for illustrative photographs and technical aid; John V. McFadden for constructional assistance; John C. Plankinton, Jr., Robert C. Lamb, James W. Sears, and Donald M. Takeuchi for help in data reduction; Mrs. Patricia Pembrook and Mrs. Laura Smothers for editorial and typing assistance; and all the members of the Atmospheric Science Branch of the Science Research Institute, Oregon State University for many helpful discussions and for providing a stimulating environment in which to work.

TABLE OF CONTENTS

LIST OF FIGURES

SURFACE OBSERVATIONS OF THE ELECTRICAL CHARGES RETAINED BY PRECIPITATION

INTRODUCTION

Firm establishment of the physical principles of cloud and precipitation formation depends on man's ability to critically observe these processes at the proper time and place. Measuring instruments carried by airplanes and sounding balloons suffer constant motion and hence have provided variable results. Radar, employing short wave length electromagnetic radiation, provides an ability to peer inside a cloud from a position miles away. The patterns presented by radar, however, are those of precipitation particles already on their trek towards earth. Consequently much of the precipitation process including the initial formation and the factors controlling the formation, remain hidden.

A different approach is the examination of the fallen precipitation for properties retained since formation. For example, micro-analysis of the entrapped particles in a raindrop can contribute knowledge of the origin of the condensation nuclei. The temperature variations during growth contribute to the history "frozen" in the structure of a snow crystal (13). This thesis reports on the examination of the electrical charge as the historical residue retained by precipitation.

THEORY

Past studies tended to treat the electrical processes of the atmosphere as a separate entity. However, they are inseparably related to the condensation and precipitation processes; indeed the difference between cause and effect has not clearly emerged (14).

Setting aside the question of the cause and effect relationship prior to the onset of precipitation, this study concerns the mechanism of continuing charge separation in precipitating cumuli and to a greater extent in thunderstorms. During the last half century the many theories put forward to explain thunderstorm electricity have in no case withstood the accumulation of more detailed information concerning storm behavior.

Simpson (13) accounted for production of electricity by the momentary contact of ice crystals during collision. The ice crystals were assumed to receive a negative charge, the compensating positive charge being carried upward on cloud droplets.

Workman and Reynolds (17) proposed in 1948 a theory of electrification based on experiments which discovered that during the freezing of dilute aqueous solutions a potential difference developed across the ice-liquid interface.

With the majority of solutions tested, the ice became negative with respect to the liquid.

Mason (12) discounts these theories. Without denying them as possible, he observed that they do not account for the charging rate required by observed thunderstorms. Thus, Mason proposed a new theory based on the preferential migration of positive ions under the influence of a temperature gradient.

H^+ and OH^- ions, formed by dissociation of a small fraction of the ice molecules, separate under the influence of a temperature gradient. This process depends on the fact that the concentrations of positive and negative ions increase rapidly with increasing temperature with the OH^- ion diffusing more slowly through the ice crystal than does the H^+ ion. Thus, a steady temperature differential across a piece of ice will result in a greater concentration of negative ions at the warm end. In the case of a freezing raindrop, a shell of ice forms on the outside of the drop. The interior proceeds to freeze at a rate determined by the dissipation rate of the latent heat. In this manner a radial temperature gradient forms as the drop cools to the air temperature. Under these conditions positive charges migrate toward the surface and leave a negative charge at the center of the drop. The drop bursts because of expansion forces created as the liquid interior freezes, and the splinters carry away the positive charges on the ice surface.

Hailstones, warmer than the supercooled cloud droplets through which they fall also separate charges with the negative charges residing on the hailstone. Charge separation occurs then as basically a thermoelectric effect.

Possibly the greater separation of electrical charges results from a precipitation particle remaining in a region of subfreezing temperatures during the growth process. The height of the source cloud provides a suggested determinant of the time spent by a precipitation particle above the freezing level.

Mason's theory and others previously described postulate negative charges on the frozen particles. If, then, these charges are retained, or at least only proportionately modified during descent, measurements of the charge polarity would indicate whether or not the rain resulted from melting an ice form of precipitation.

A comparison of the negative to positive charge ratio of precipitation with cloud height above the freezing level should disclose whether earth based instruments can discern the initial charge pattern.

INSTRUMENTATION

To test the above hypothesis and to provide additional information concerning the electrical properties of the atmosphere, the author designed, and with the aid of Atmospheric Science Branch personnel, constructed a precipitation charge electrometer and a point discharge current meter.

The precipitation charge electrometer, shown schematically in Figure 1, consists basically of an electrostatically shielded collector, charge sensor, amplifier, and chart recorder. The precipitation falling into the collector deposits its characteristic charge on the surface. There a static charge sensing electrometer detects it. An amplifier then provides sufficient gain to drive the writing pen of the chart recorder.

The wooden box containing the collecting funnel and measuring apparatus has a total covering of copper screen, soldered at all seams, to provide good electrostatic shielding. Low conductivity polystyrene spacers separate the collector, a standard U. S. Weather Bureau 8" tipping-bucket raingage, from the box. A truncated metal cone placed over the funnel opening provides collimation, splash prevention, and additional electrostatic shielding.

The static field sensor, a high input impedance (10^{-14} amperes grid current) electrometer tube, converts the varying

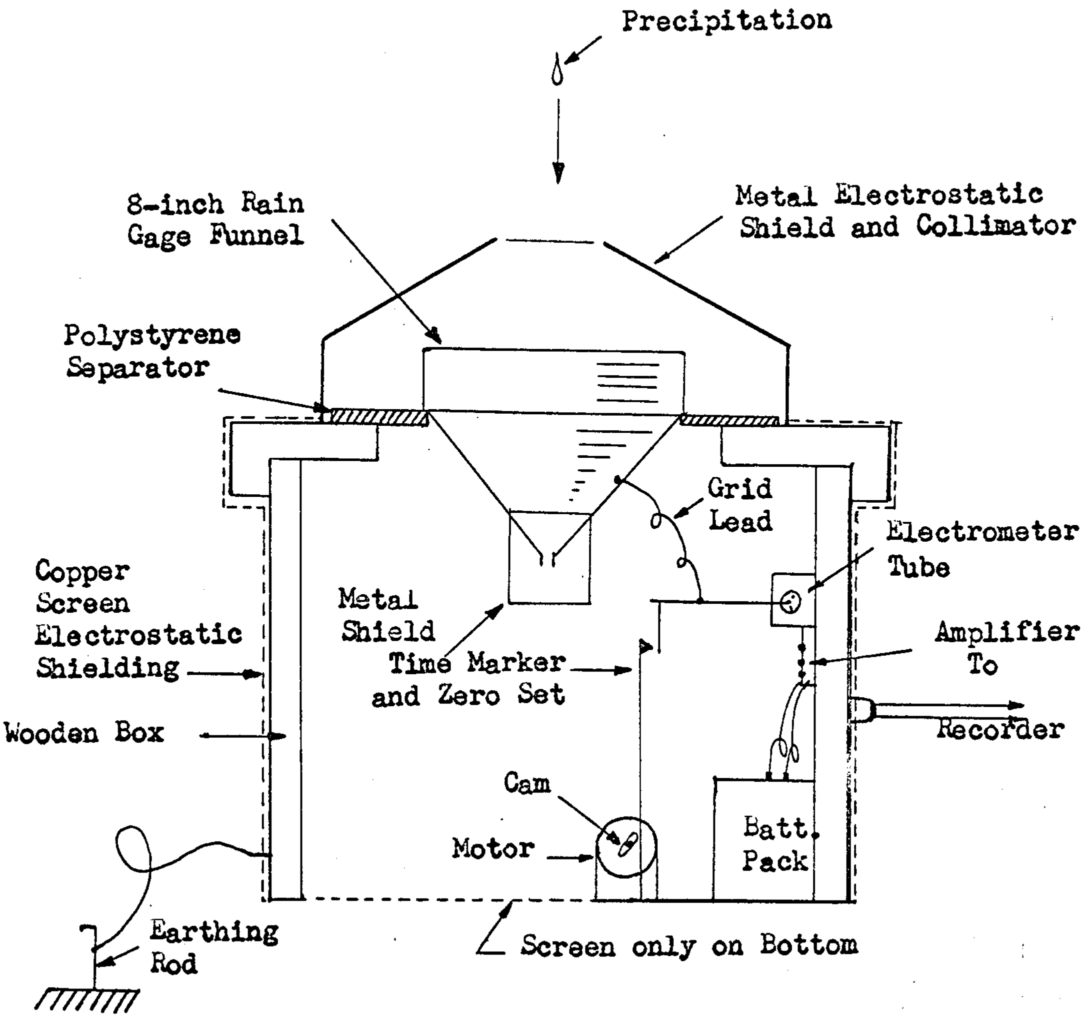

Fig. 1 PRECIPITATION CHARGE ELECTROMETER CONSTRUCTION

static electric field to a varying electric current. A differential amplifier amplifies the varying current and then converts it to a lower impedance to drive the remotely located chart recorder.

The combination of the low voltage plate operation of the electrometer tube and the ordinarily low voltage transistor amplifier and driver permit common battery operation with small power demands. The minimum temperature drift design of this circuit (Figure 2) should provide hundreds of hours of trouble-free field use under normal ambient operating conditions.

A small electric motor drives a cam operated switch which earths the input of the measuring circuit every fifteen seconds. This provides a timing mark, a zero level on the chart of the recorder, and drains any residual charge on the collector to earth. An earthing lead attached to the box shielding connects to a rod driven into the earth at the location.

The circuit has an input time constant of approximately fourteen seconds and a response time of two milliseconds. The input conductance and capacitance define the time constant, while the recording pen determines the response time. Lowering the input resistance resulting in a time constant of 0.7 seconds, and reducing the collecting aperture from 50 square inches to 25 square inches reduced the static charge build-up during periods of intense rainfall.

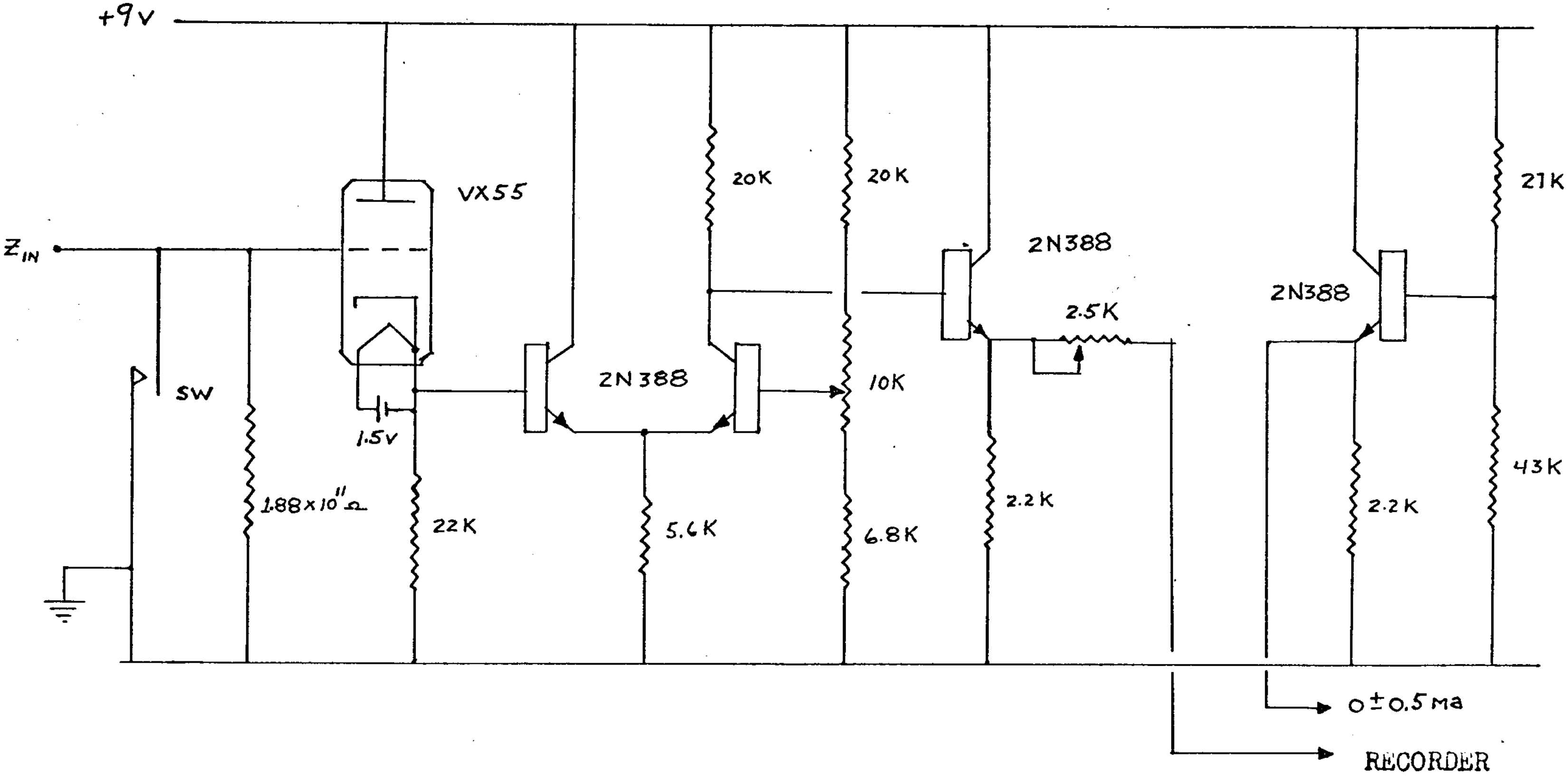

Fig. 2 PRECIPITATION CHARGE ELECTROMETER CIRCUIT

The precipitation electrometer has a sensitivity of 2.0×10^{-4} esu (0.7×10^{-13} coulomb) and a range of $\pm 3.3 \times 10^{-2}$ esu (1.1×10^{-11} coulomb). The accuracy of the electometer-recorder system is ± 10 percent of the chart reading.

The 8" tipping-bucket raingage also provides a measure of the total rainfall on a separate recorder as shown in Figure 3.

Figure 4 shows the precipitation charge electrometer in the field.

Figure 5 outlines the method of measuring the corona or point discharge current. A high-gain direct current amplifier amplifies the voltage drop across a one ohm resistor located approximately four feet from the top of a 40 foot antenna. The top of the antenna has a sharp point, thus increasing the electric field gradient and facilitating the flow of current into the atmosphere. The signal generated across the one ohm resistor travels to the high-gain D. C. amplifier via coaxial cable. The amplifier provides sufficient power to actuate a chart recorder with a sensitivity of 0.5 milliamperes.

Figure 6 shows schematically the electronic circuit of the amplifier. High gain circuits of this type generally suffer electrical drift, caused largely by thermal variations in the surrounding environment. To compensate for the inherent drift, the design

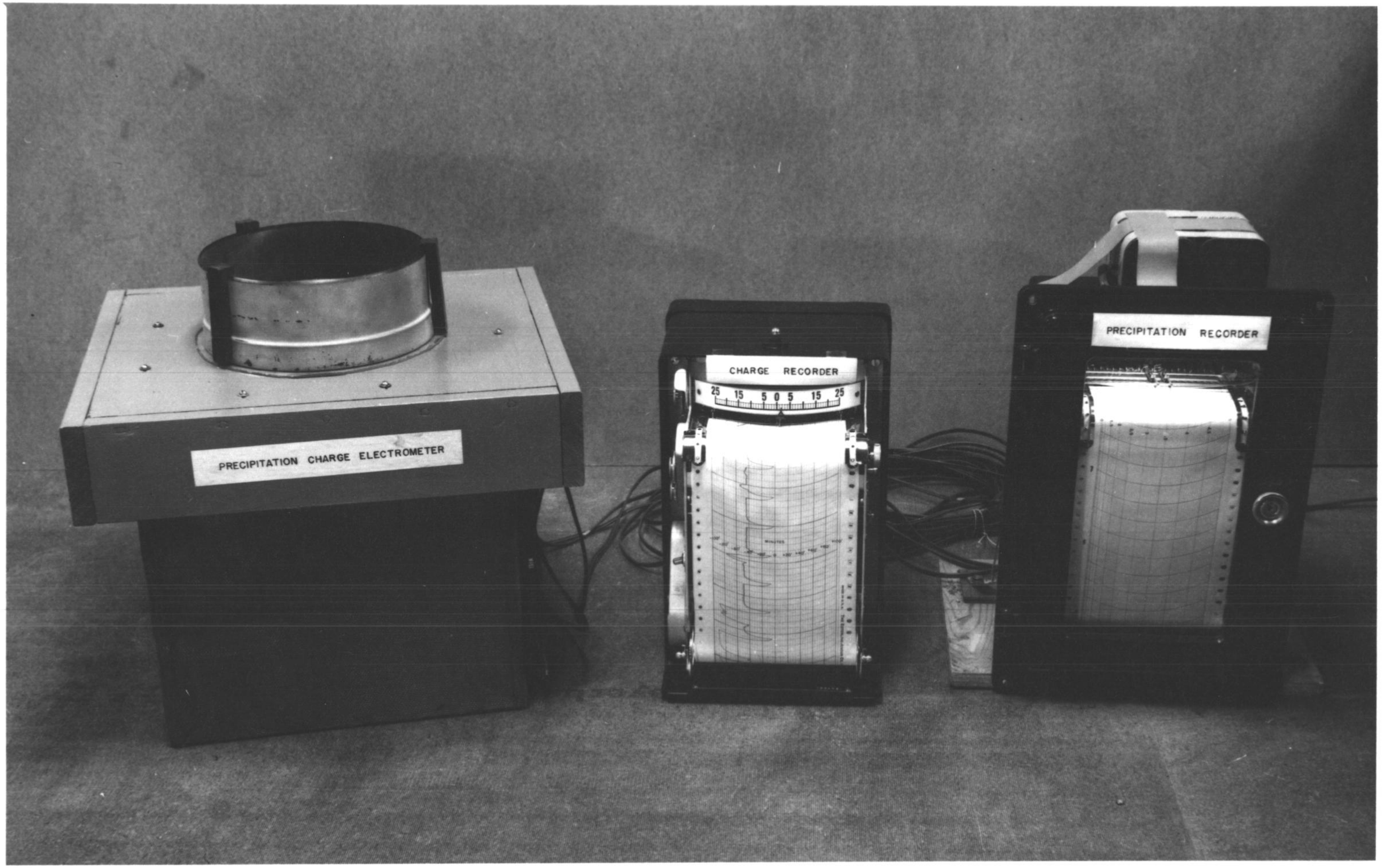

Fig. 3 PRECIPITATION CHARGE ELECTROMETER SYSTEM

Fig. 4 PRECIPITATION CHARGE ELECTROMETER IN THE FIELD

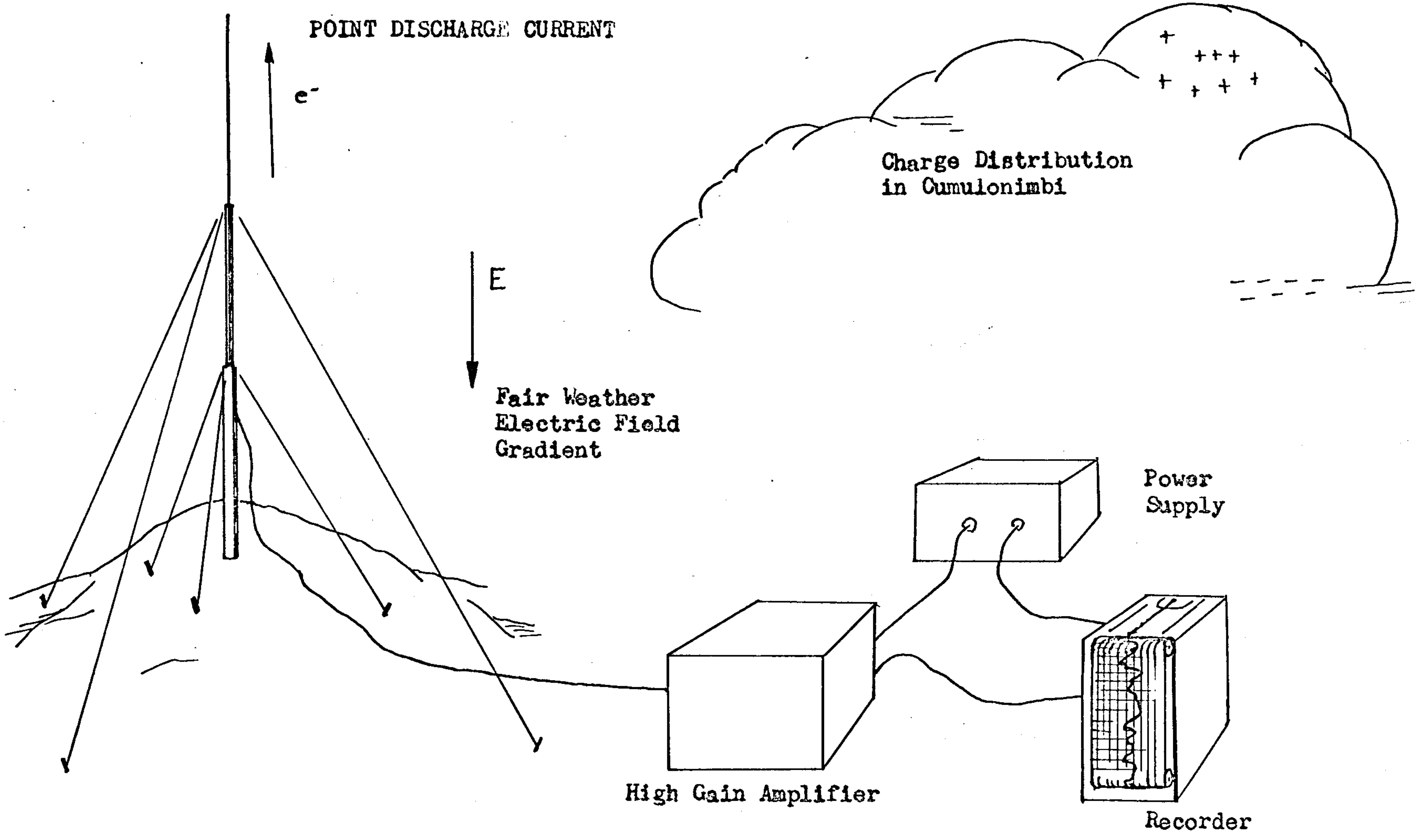

Fig. 5 POINT DISCHARGE CURRENT MEASURING SYSTEM

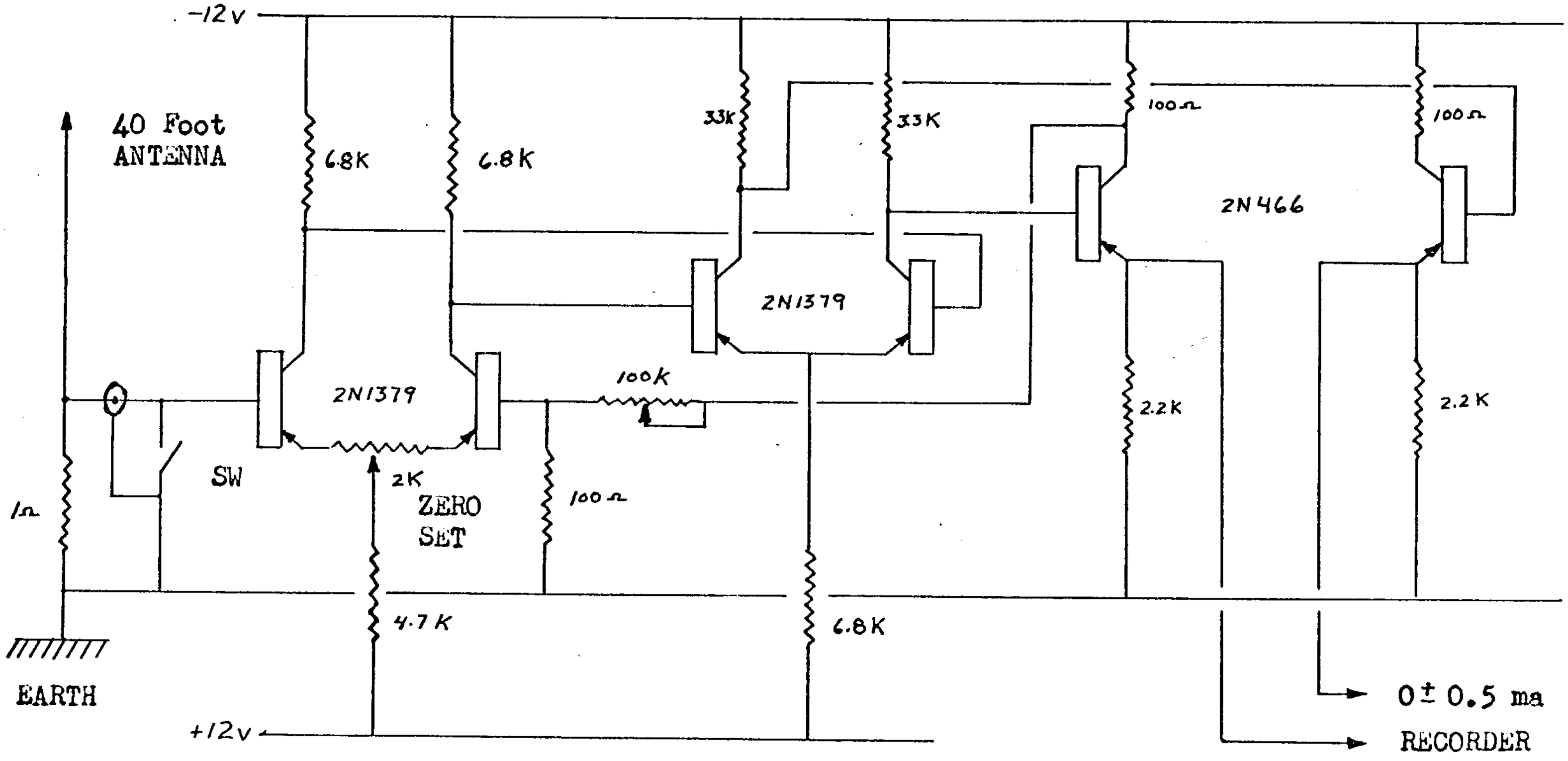

Fig. 6 POINT DISCHARGE CURRENT AMPLIFIER

includes a negative feed-back loop. This results in a long-term stability of better than ± 0.5 millivolts per hour. A cam-operated switch earths the input approximately every ten seconds to provide a zero reference mark on the recording chart. The system can resolve changes in point discharge current of two microamperes. Esterline Angus chart recorders with a full scale deflection of ±0.5 milliamperes recorded the output of both the precipitation charge electrometer and the point discharge current meter.

Observers took raindrop distribution measurements using the methylene blue impregnated filter paper technique. Assistants counted by hand the dyed blots caused by the raindrops and determined their sizes using a transparent overlay size gage.

A 3.2 cm wavelength Radar Set AN/CPS-9 recorded precipitation echo heights above the precipitation electrometer. This radar, located atop McCulloch Peak approximately 5.7 miles from the precipitation recorder supplied range height (RHI) indications of precipitation echoes at approximately ten minute intervals on March 2 and March 27 through 30, 1963. Figure 7 shows the AN/CPS-9 antenna and the 40 foot Point discharge current antenna.

On March 29 and 30 a vertically pointing 3.2 cm radar OS/APR-21 atop Covell Hall on the Oregon State University campus provided continuous precipitation echo heights (16). Photographic

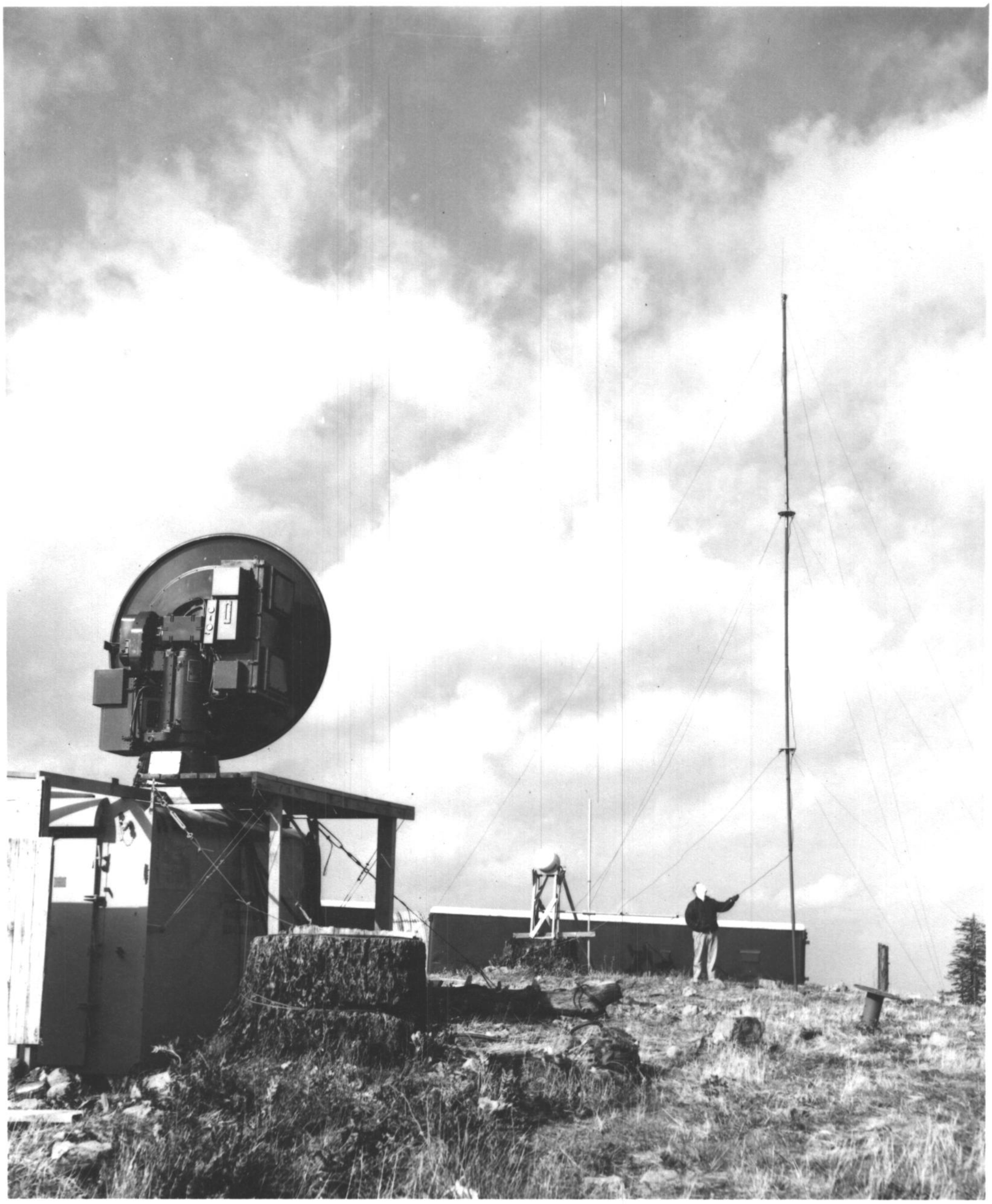

Fig. 7 RADAR ANTENNA AND POINT DISCHARGE ANTENNA ATOP McCULLOCH PEAK

scope display recorders on both radars provided permanent records of the precipitation echo heights.

The U. S. Weather Bureau office at Salem, Oregon furnished atmospheric soundings at 1500Z and 2300Z on the days of observation.

Observers made measurements of wind velocity and direction, temperature, pressure, humidity, and rainfall on site. The continuous recording weather instruments in the Physics Chemistry building on the Oregon State University campus provided supplementary data.

SYNOPTIC CONDITIONS

Comprehensive data obtained on March 2, 1963 and during the period from March 27 through 30, 1963 allowed reliable analysis and comparison.

Synoptic analysis for March 2 showed that a cold front moved across Oregon two days prior to the investigation and brought a maritime polar air mass which dominated throughout the investigation period. A high pressure system off the southern coast of Oregon, acting with a low pressure area on the southern Alaska coast, resulted in upper winds from the west-northwest.

The 2300Z Salem sounding showed a moist air mass with conditional instability in the lower layers and a freezing level of 3000 feet. Records showed a 43°F temperature with 84 percent relative humidity, light and northerly winds, and cloudy skies with rain showers west of the Cascades.

On the morning of March 27, a low pressure area off the southwest coast of Oregon began to intensify and move toward Oregon, replacing a maritime polar air mass. The resulting low and the indistinct occluded front dominated the synoptic situation until frontal passage at 1800 PST. Air flowed generally from the south to southwest in the morning. The afternoon sounding revealed a moist but fairly stable atmosphere with a freezing level of 6000 feet. Surface temperatures continued slightly below seasonal, with little temperature change after frontal passage. Clouds with moderate precipitation predominated during the afternoon and early evening.

At approximately 2300 PST another occluded front passed over Oregon while still another passed over at 1100 PST on March 28. The passage of many lines of precipitation on the 28th provided the significant difference in weather from the previous day. The barometer remained low under considerably unstable conditions with values averaging 1/2 inch lower than on the days prior to the 27th. Strong surface winds blew with gusts to 70 miles per hour in places. The 1100Z sounding showed dryer air aloft with conditional instability in the lower layer and a freezing level of 3600 feet.

The weather of the 29th remained under the influence of maritime polar air. Afternoon and evening winds blew generally from the west. The 2300Z soundings showed conditional instability present with considerable moisture aloft and a freezing level of 3600 feet. In the late evening of the 29th and early morning of the 30th, the barometer showed large instability due to line passages. Short heavy showers predominated until late in the morning of the 30th. The freezing level dropped to 3400 feet at the time of the 1100Z sounding.

DATA

The Esterline Angus chart recorder graphically recorded the magnitude and polarity of the precipitation charge. For analysis, the author sectored the recording into two-minute periods with readings of the magnitude and polarity taken at two-second intervals, thus giving sixty possible samples per period. Extension of the interval to four minutes provided a more reliable statistical sample at times of light or questionable precipitation. A tabulation then facilitated analysis of the data in each two-minute time sequence under the following headings:

1) Total number of positive drops
2) Total number of negative drops
3) Total number of positive drops of a given magnitude
4) Total number of negative drops of a given magnitude
5) Total number of drops of an absolute magnitude
6) Largest positive charge per period
7) Largest negative charge per period
8) Ratio of negative to positive drops per period

A sample of this data is shown in Appendix I.

On March 2 the tabulation shows maximum positive and negative charges of $+11.0\times10^{-3}$ esu and -43.7×10^{-3} esu respectively. During the line passage on March 30 at 0100 PST $+46.0\times10^{-3}$ esu and -35.0×10^{-3} esu appeared as the corresponding maxima. Maximum positive and negative charges for the five days examined averaged approximately $\pm20.0\times10^{-3}$ esu. The positive and negative charge for the total rain analyzed for the five day period averaged approximately $+4.5\times10^{-3}$ esu and -4.2×10^{-3} esu respectively. The analysis sampled only the heavier showers, therefore, resulting in higher averages than normally expected for continuous period sampling. In general more positive than negative rain fell, apparently agreeing with observations of other researchers in atmospheric electricity (10)(13).

The author read point discharge currents from the recording in a similar manner but plotted them directly as a graph to give a time-compressed picture of the entire recording period.

Time lapse photographs of the AN/CPS-9 radar RHI scope, taken at the same time as the charge recordings, furnished direct measurements of the precipitation echo heights. A continuous film provided by the vertically pointing radar recorded precipitation echo heights on the evening of March 30, 1963. The analyzer samples this film at ten-second intervals and plotted it to give a continuous time-compressed picture of the precipitation echo height.

Assistants in the Atmospheric Science Branch counted and tabulated the raindrops. Normalization of these distributions by the ratio of the filter paper and charge collector areas and the ratio of the exposure times permitted statistical comparisons. The author then plotted a function of the ratio of the number of negative drops to the number of positive drops against the cloud height for a "continuous" 50 minute period on March 30, 1963. Fourteen selected samples of charge ratios covering the four day period from March 27 to March 30, 1963 appear plotted against precipitation echo height in Figure 10.

The statistical techniques of linear regression analysis provided a method of arriving at a quantative measurement of the interrelationships between the two variables (5). Regression line parameters determine the relationship of the equation. The square of the correlation coefficient gives a measure of the relative amount of variation in the dependent variable that is explained by the independent variable.

The author compared a function of the absolute charge on the raindrop to the raindrop size distribution and after determination of a "best fit", he took five samples on five different days to compare statistically using the same relationship.

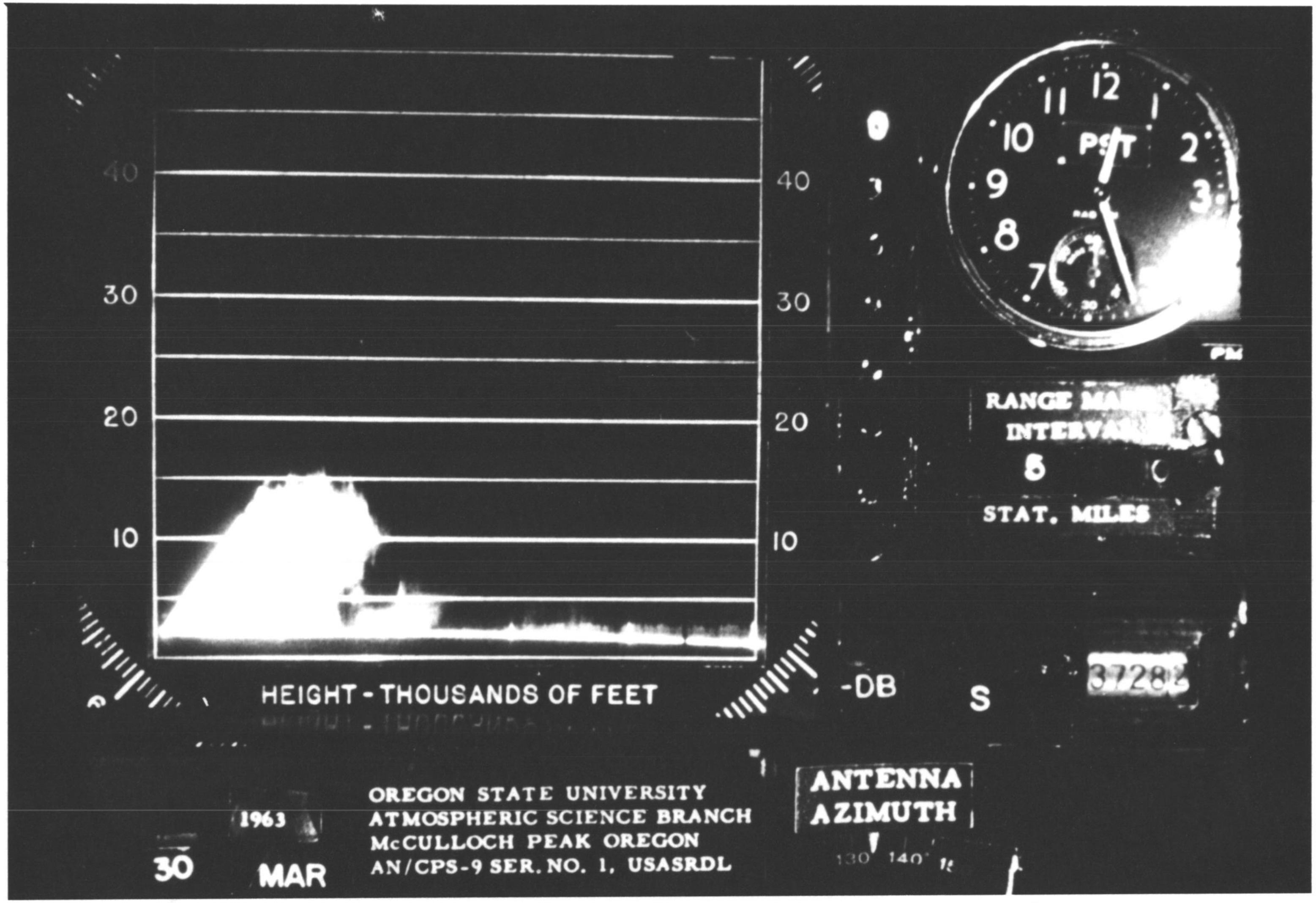

Fig. 8 RHI RADAR PHOTOGRAPH OF THE LEADING EDGE OF A LINE OF PRECIPITATION

DISCUSSION

Point discharge currents, recorded for the entire period, for the times of precipitation charge recordings, March 27 through March 30, 1963 show a point discharge current very nearly steady at approximately 9 - 14 microamperes. Positive current flowed into the pole, i. e., electrons flowed from the mountain to the atmosphere. The current did not reverse and showed only slight increases and decreases associated apparently with wind variations. During this time, precipitation charges had varying magnitudes, intensities, and polarities. This agrees with the conclusions of Gunn and Devin (9) that no relationship exists between point discharge current and rain charge.

Observers reported hail, snow, and the sounds of thunder on the evening of March 28, 1963. During this time exceptionally large point discharge currents exceeding 600 microamperes were measured. Multiple lightning strokes with normal field recovery times occurred, but no evidence appears of expected field reversals (11).

Possible explanations of these measurements include these two: 1. The orographic and maritime influences tend to diffuse the charge centers which occur in "normal" cumulonimbus. 2. In effect the corona point atop McCulloch Peak provides the terminating

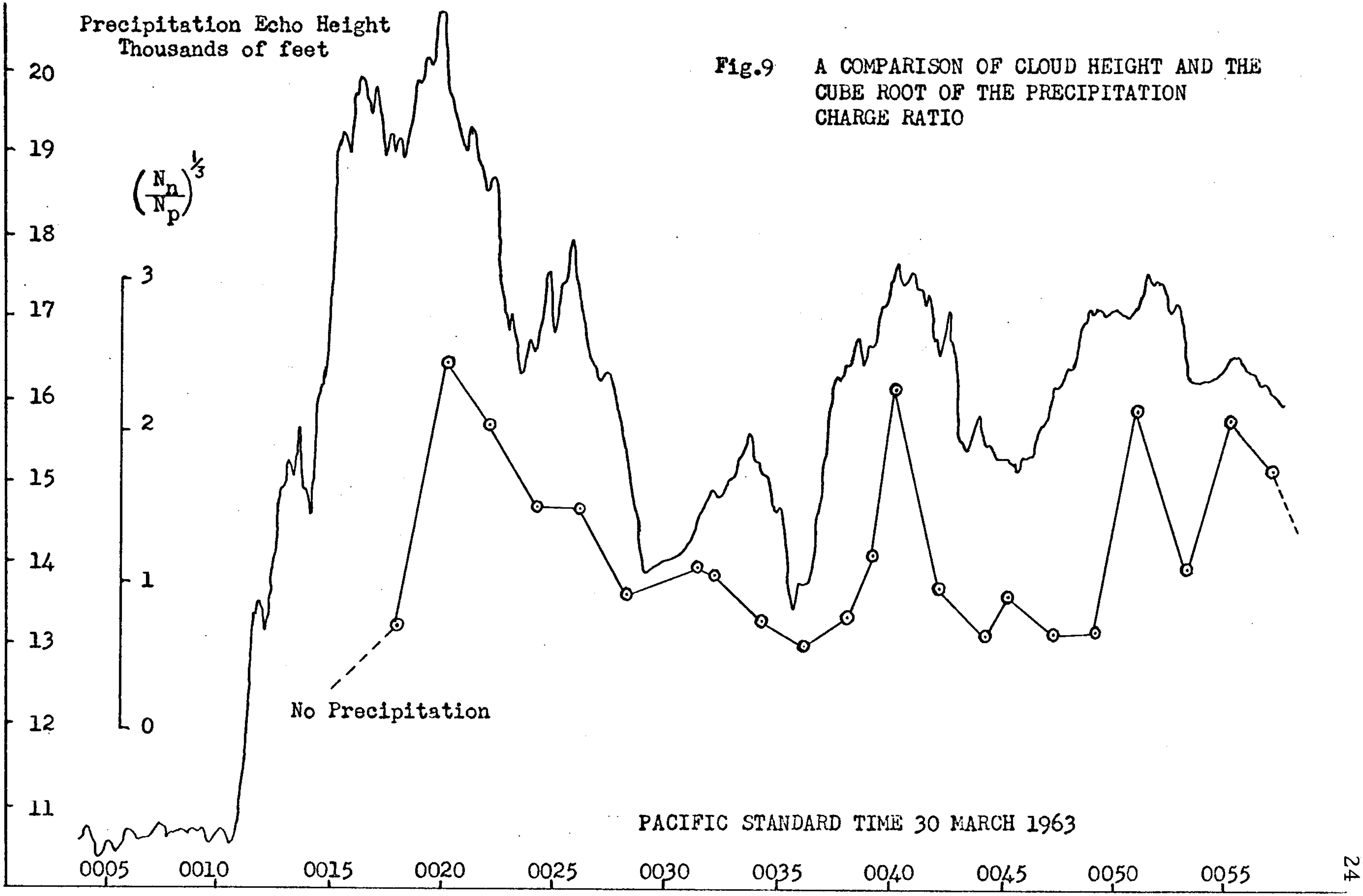

Fig.9 A COMPARISON OF CLOUD HEIGHT AND THE CUBE ROOT OF THE PRECIPITATION CHARGE RATIO

point for the entire mountain. One may expect that mountain currents would have a certain amount of "electrical inertia", a distributed resistance-capacitance effect which could tend to support the current flow in the absence of a field gradient and might even sustain is through a short-time field reversal. The data shows no unusual variations in precipitation charge during this period.

Operation of the vertically pointing radar enabled a continuous 50-minute comparison of the precipitation echo heights and precipitation charge polarity ratio. The 50-minute comparison period covers the passage of a line 15 miles wide moving at a line velocity of 15 miles per hour across the site of the precipitation charge electrometer. Figure 8 shows the leading edge of this line March 30 at 0026Z as it appeared on the RHI scope of the AN/CPS-9 radar set.

Figure 9 shows echo height with time compared to the cube root of the ratio of the number of negative drops to the number of positive drops. The ratio of the number of negative to positive drops appears instead of the number of a given magnitude since the author believes that the magnitude depends more on the trajectory than does the number of drops of a given charge sign. For example, a large positive drop will, on the average, break into about the same number of smaller drops while falling as will a large negative drop. The ratio, therefore, remains the same. However, the loss or gain of charge by a drop in falling through a gradient field depends on size, thereby changing the original ratio. The cube root in this analysis provides a convenient ratio only. Other powers would merely tend to reduce or exaggerate the contour. Statistical comparison at 22 points gives a correlation coefficient of 0.61, the charge ratio, therefore, showing a 37 percent dependency on cloud height.

In comparing the two curves, the author computed mean fall times for the measured drop sizes. From heights of 20,000 feet drops fall to the ground in 15 minutes. Offsetting the two curves by this amount of time destroys all vestiges of correlation. Best fit occurs with the curves within ±2 minutes of each other, a value less than the uncertainty of synchronization of the timers on the charge recorder and the radar. This indicates cloud or cell persistence. The cloud evidently maintains its vertical identity for periods greater than the precipitation fall time.

Figure 10 shows a cloud height-charge comparison for 14 time periods over four days. The lines connecting the points permit comparisons only, since the points are completely independent. Not randomly selected, these samples occurred when the charge measurement allowed a large number of samples for a given period and

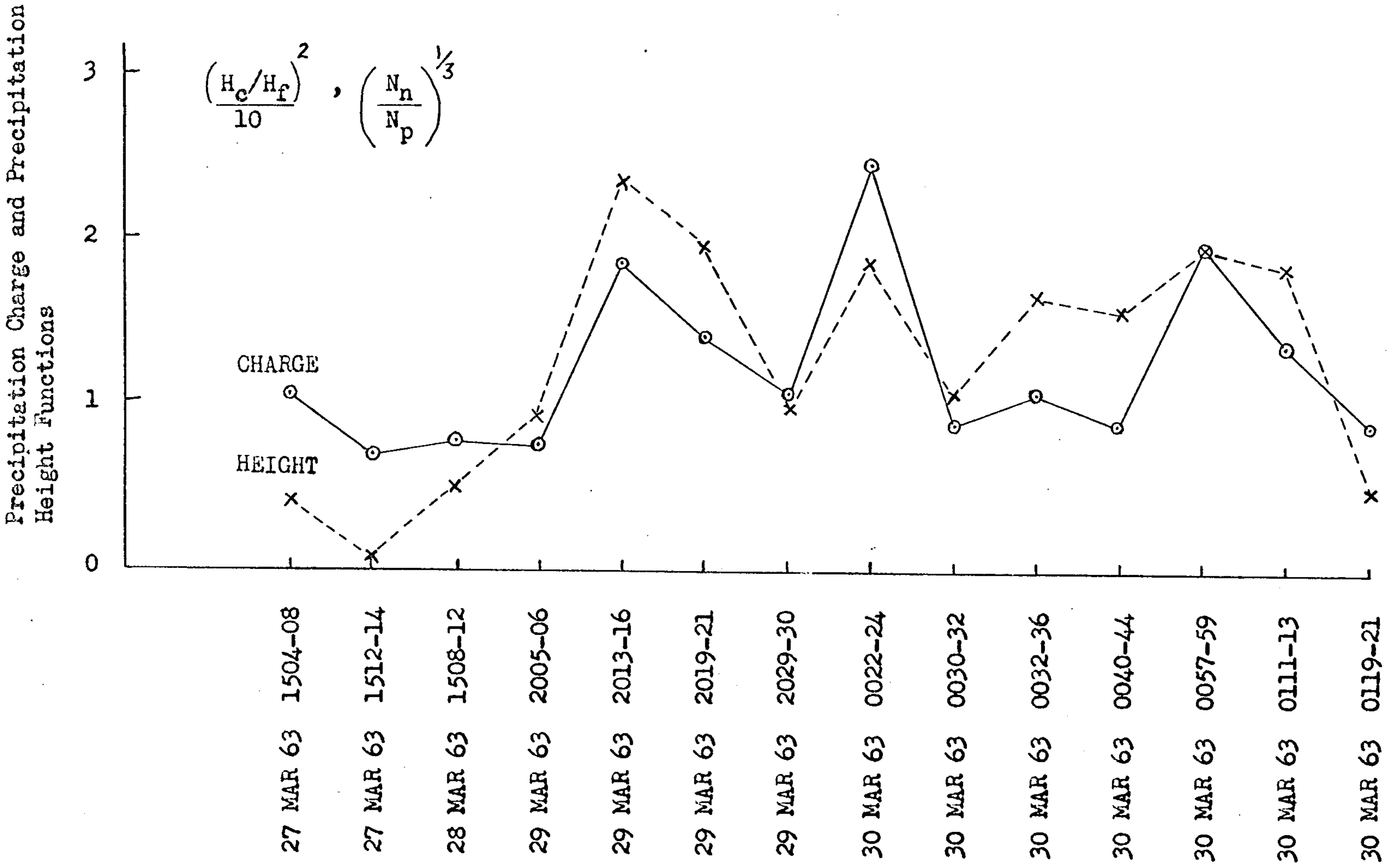

Fig. 10 A COMPARISON OF FUNCTIONS OF PRECIPITATION HEIGHT AND PRECIPITATION CHARGE DURING A FOUR DAY PERIOD

when the radar precipitation height remained constant over the charge recorder for periods of time comparable to the precipitation fall time. The comparison used "normalized" cloud heights for the four day period determined by dividing actual height by the freezing level height determined from the Salem, Oregon radiosonde soundings. After scale adjustment, statistical analysis showed a correlation coefficient of 0.74 or a charge ratio dependency on cloud height - freezing level of 54 percent and the following equation of best fit:

$$\left(\frac{H_c}{H_f}\right)^2 = 5.4 + 5.2 \left(\frac{N_n}{N_p}\right)^{\frac{1}{3}}$$

where:

H_c = cloud height

H_f = freezing level

N_n = number of negative drops

N_p = number of positive drops

According to the equation, if the freezing level should drop to the surface, all the drops should have negative charge. In general this does not occur (4). Nor does there always appear a mixture of negative and positive drops. A more satisfactory equation would have the form:

$$\left(\frac{H_c - H_f}{H_c + H_f}\right)^A = B + K^C \left(\frac{N_p - N_n}{N_p + N_n}\right)^D$$

with the constants A, B, C, D, and K dependent on geographical location and atmospheric conditions.

The charges on raindrops measure about one order of magnitude smaller than that necessary to produce corona on a spherical drop (8). However, the charges approximate those expected on irregularly shaped drops. If this is the case, the absolute charge of each drop would relate to the drop size. Figures 11 and 12 show a comparison of the distribution of the cube root of the absolute charge and the drop size distribution. An alternate method giving the same results would compare the drop area (or diameter cubed) with the absolute charge.

Because of the sampling technique used to arrive at a charge distribution, the number of drops varies linearly with the total counted in the filter paper technique. The resulting constant of proportionality corrects the number scale. The fact that the drops splash on impact decreases the reliability of the drop size distribution on the small drop (lefthand) end of the scale. The drop size distribution at the large diameter end of the scale depends on the chance encounter of one or two large drops, a fact which also decreases its reliability. Statistical comparison of the curves of Figures 11 and 12 only in the more reliable center area of the distribution gives correlations of .98 and .96 respectively, or better than 90 percent interdependency. Samples taken on five different

Fig. 11 A COMPARISON OF RAINDROP DISTRIBUTIONS DETERMINED ELECTROMETER MEASUREMENTS 1650 PST 2 MARCH 63

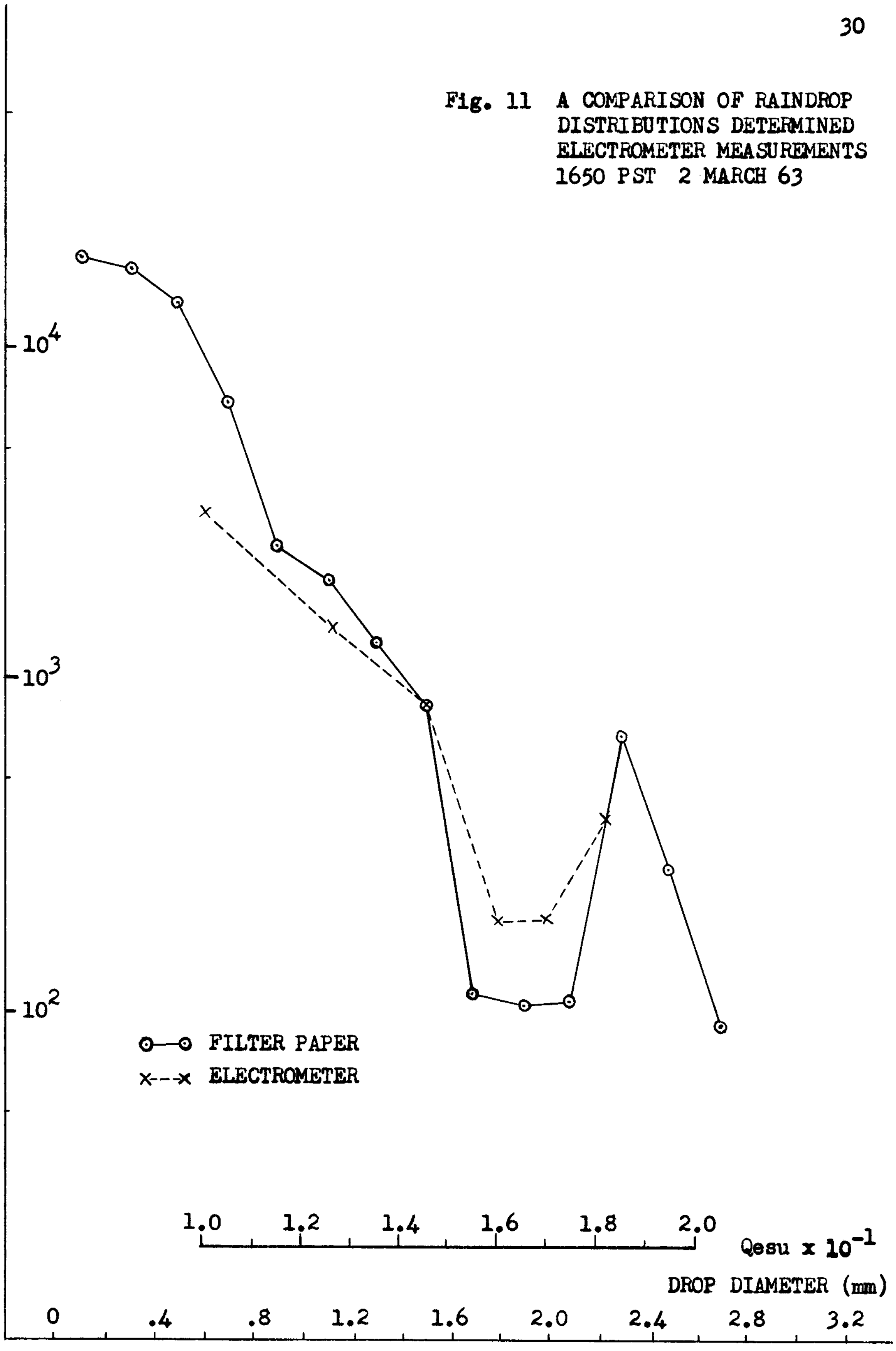

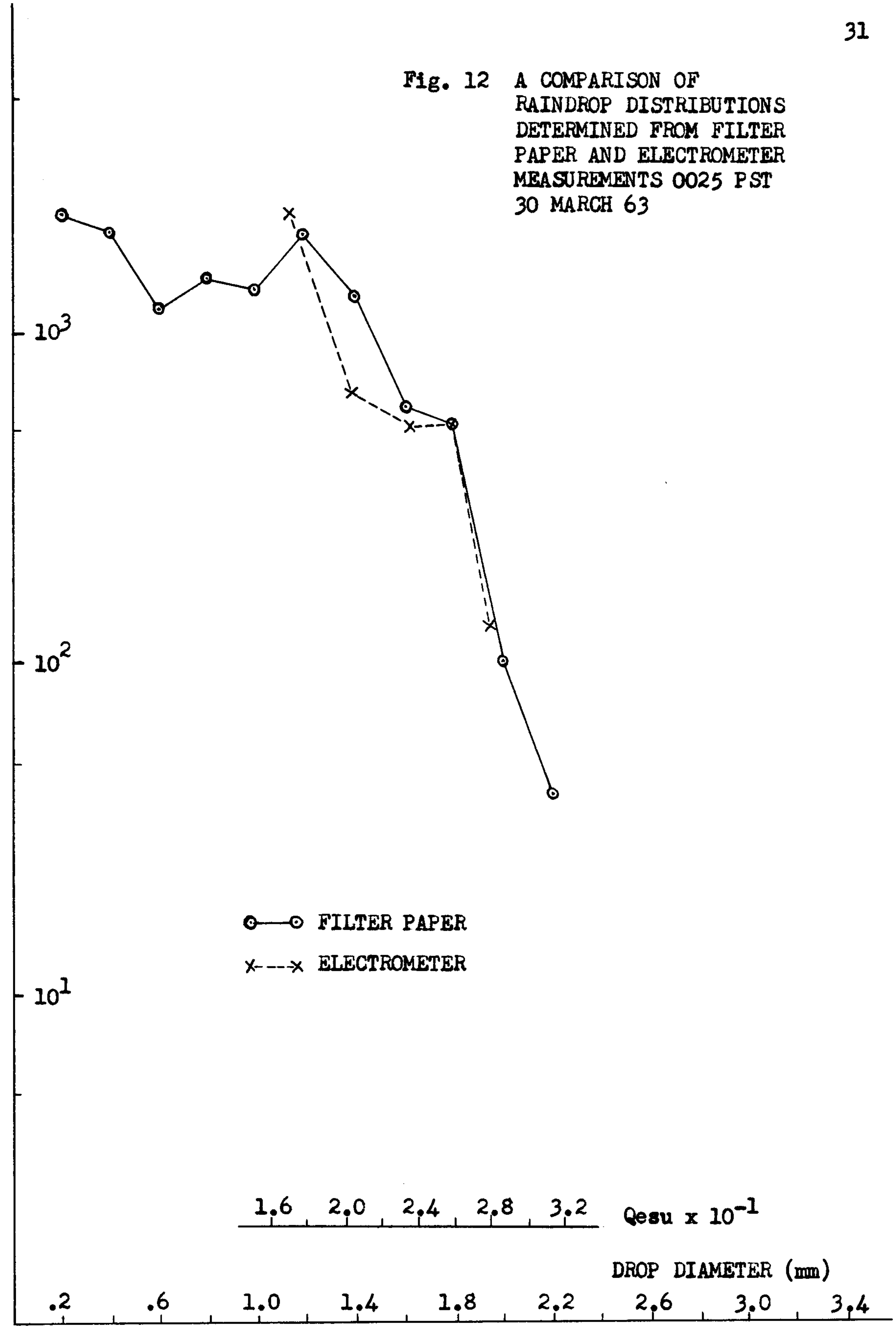

Fig. 12 A COMPARISON OF RAINDROP DISTRIBUTIONS DETERMINED FROM FILTER PAPER AND ELECTROMETER MEASUREMENTS 0025 PST 30 MARCH 63

days give a correlation for the total of r = 0.67 or a 45 percent interdependency.

Certain of the samples, although taken simultaneously, involved separation by approximately 100 hundred feet. At the recording rate used on the precipitation electrometer recorder the larger drops tended to cover the smaller drops during periods of intense rain. Therefore, the strength of the correlation depends somewhat on the proximity of the samplers and on rainfall intensity.

An equation which describes the suggested charge - drop size relationship has the form:

$$N_d = A\ 10^{B^c}|Q|^{\frac{1}{3}}$$

where: N_d = the number of drops of a given diameter

A = A constant dependent on sampling rate

B = A proportionality constant between charge magnitude and drop size

Q = Absolute magnitude of the charge

c = Atmospheric condition factor

The constancy of charge with drop size indicates that either the drop will support no more charge without corona discharge or that the drops experienced a constant charging rate during formation.

Drop charge distributions show a bimodal distribution in four of the five cases examined. This agrees with Sarmah's (15) findings on drop distributions in western Oregon.

A qualitative comparison of radar precipitation echo heights, rain intensity, and charge ratio shows that in general the greater rain intensity and the larger negative-to-positive charge ratios occur near the leading edge of the precipitation echoes.

SUMMARY

Present existing theories of precipitation electrification suggest that the larger frozen precipitation particles acquire a negative charge during formation. The author designed a point discharge current meter to provide information to show that precipitation charges are independent of point discharge current. He also designed and constructed a precipitation charge electrometer to measure the charges retained by precipitation at the earth's surface.

The measured charges compared with cloud heights for a continuous 50-minute period and as samples over a four day period show a statistical interdependency of 37 percent and 55 percent respectively. A comparison of charge magnitude and drop size data from five sample periods show a 45 percent interdependency. Qualitative observations show that: 1) the drop size variations as determined from charge measurements are bimodal; and 2) that the more intense rain and the higher percentage of negative drops occur near the leading edge of the precipitation echoes.

CONCLUSIONS

In general, the prototype instruments performed satisfactorily in measuring the atmospheric electric parameters of precipitation charge and point discharge current. The instruments need improvements in dynamic range and general construction.

Of the cases analyzed, the electrical charges retained by precipitation have a distribution in time and polarity showing a definite relationship between cloud height and charge ratio and between drop size and absolute charge magnitude. This indicates that the surface observations of the electric charges retained by precipitation are dependent on the source of the precipitation. If substantiated, these findings will provide the research meteorologist and cloud physicist with a new tool for studying the mechanisms of precipitation.

Referring to the radar photograph (Figure 8) of a precipitating cell and remembering that in general the radar echo shows only the precipitation and not necessarily the cloud structure surrounding the precipitation, the reader can envision a cloud forward and above the echo. If, then, air flows inward and upward at approximately the 5000 foot level, the precipitation particles at the forward edge of the cloud would tend to be sustained at higher elevations longer and grow larger than those toward the rear of the cloud. Likewise, the reader may envision a cloud arranged symmetrically about the precipitation echo with air entering the bottom and rising through the center to sustain large drops during the cloud growth stage. Shearing of the cloud top during the mature and dissipation stages will tend to carry the precipitation downward and toward the front of the cloud. Either mechanism could explain the drop size and drop distribution observed on the surface.

These results could substantiate either the Byers (2) or Ludlam (1) models of the thunderstorm. However, atmospheric conditions reported by other researchers reveal cloud heights of 30,000 to 50,000 feet, bases near 4,000 to 10,000 feet and thicknesses of thousands of feet. Clouds in western Oregon during this study had heights typically 8,000 to 20,000 feet with bases 800-2500 feet high and precipitating cloud layers sometimes only hundreds of feet in depth. The presence of maritime and orographic influences, the differences in raindrop size distribution, and the electrical evidence previously cited all tend to show a dissimilarity in cloud structure between that generally cited in the literature and that studied at Oregon State University.

For these reasons the author refrains from fitting the evidence to an established model, preferring to look upon it as a coastal cloud phenomenon - a class in itself - until further research more sharply delineates the model which the evidence prescribes.

A precipitation particle, during its flight towards earth may colide, splinter, freeze, pass through regions of strong electric gradients, encounter ions, and many other environmental anomalies, all of which tend to modify the original origin-dependent electric charge.

Geographical differences in atmospheric conditions previously described would increase the probability of modifications to the original charge patterns. For this reason, one probably cannot extrapolate these results to other geographical areas without modification.

SUGGESTIONS FOR FUTURE RESEARCH

The author believes the implications suggested by this research warrant verification. To determine the modifications of the charge on the drop while falling through the atmosphere, the author proposes to construct at least three precipitation charge electrometers, placing them in a line on the windward slope of a mountain such that, as nearly as possible, they would sample the same precipitation at different heights. Under certain conditions, this could achieve simultaneous measurements of the precipitation charge both above and below the freezing level. This could also provide measurements at the precipitation origin or place of formation inside the cloud as it encompasses the mountainside recording sites. This method would at least partially eliminate many of the questionable parameters in the above research.

For better statistical data collection, an apparatus similar to that used by Gunn (7) would improve the raindrop size-charge relationship data. His apparatus simultaneously measured raindrop charge and size. The drops passed through an induction ring and then impacted on a continuously moving filter paper belt.

The maritime-orographic affects on the point discharge current cause anomalies which need further investigation.

A most intriguing speculation arises in the question, "What natural weather modification occurs because of point discharge currents emitted by the mountains of the Coast Range as maritime air masses waft over them?" This could provide interesting research.

BIBLIOGRAPHY

1. Battan, Louis J. Cloud physics and cloud seeding. New York, Doubleday, 1962. 144 p.

2. Byers, Horace Robert. General meteorology. New York, McGraw-Hill, 1959. 540 p.

3. Chalmers, J. Alan. Atmospheric electricity. London, Pergamon, 1957. 327 p.

4. Chapman, S. Thundercloud electrification in relation to rain and snow particles. In: Horace Robert Byers' Thunderstorm electricity. Chicago, University of Chicago, 1953. p. 207-230.

5. Duncan, Acheson J. Quality control and industrial statistics. Homewood, Illinois, Richard D. Irwin, 1955. 344 p.

6. Fletcher, N. H. The physics of rainclouds. Cambridge, Cambridge University, 1962. 385 p.

7. Gunn, Ross. Electronic apparatus for the determination of the physical properties of freely falling raindrops. Review of Scientific Instrumentation 20:291-296. 1949.

8. ____________________. The free electrical charge on thunderstorm rain and its relation to droplet size. Journal of Geophysical Research 54:57-63. 1949.

9. Gunn, Ross and Charles Devin, Jr. Raindrop charge and electric field in active thunderstorms. Journal of Meteorology 10:279-284. 1953.

10. Humphrey, W. J. Physics of the air. New York, McGraw-Hill, 1940. 675 p.

11. Kitagawa, N. and M. Brook. A comparison of intracloud and cloud-to-ground discharges. Journal of Geophysical Research 65:1189-1201. 1960.

12. Mason, B. J. Clouds, rain and rainmaking. Cambridge, Cambridge University, 1962. 145 p.

13. ________________. The physics of clouds. London, Clarendon Press, 1957. 481 p.

14. Moore, C. B., Vonnegut and A T. Botka. Results of an experiment to determine initial precedence of organized electrification and precipitation in thunderstorms. In: Leslie G Smith's Recent advances in atmospheric electricity. New York, Pergamon, 1958. p. 333-360.

15. Sarmah, Suryya K. A radar and synoptic study of rain at a point. Master's thesis. Corvallis, Oregon State University, 1963. numb. leaves.

16. Sutton, Robert W. Design criteria, construction and evaluation of a medium power weather radar system. Master's thesis. Corvallis, Oregon State University, 1959. 52 numb. leaves.

17. Workman, E. J and S. E. Reynolds. Structure and electrification. In: Horace Robert Byers' Thunderstorm electricity. Chicago, University of Chicago, 1953. p. 139-150.

Time PST 30 Mar 63	Number and Magnitude of Charges $Q \times 10^{-3}$ esu: Positive																Negative															
	35.2	33.0	30.8	28.6	26.4	24.2	22.0	19.8	17.6	15.4	13.2	11.0	8.8	6.6	4.4	2.2	2.2	4.4	6.6	8.8	11.0	13.2	15.4	17.6	19.8	22.0	24.2	26.4	28.6	30.8	33.0	35.2
0047-49															0	9	4	1	1	0												
49-51														0	1	14	3	0	1	0												
51-53												0	1	5	4	5	4	0														
53-55												0	1	0	1	0	11	7	2	0												
55-57															0	5	4	2	0													
57-59												0	1	0	0	2	8	8	3	1	1	0										
59-01											0	2	1	0	0	1	2	1	2	2	2	1	3	0	4	1	1	0	0	1	0	
0101-03										0	1	2	0	4	1	5	2	0	0	1	1	1	2	1	1	1	1	0	1	0		
03-05							0	1	0	0	0	2	2	3	3	10	2	2	0													
05-07						0	1	2	0	5	3	3	1	3	2	3	1	0	1	0												
07-09												0	2	2	5	9	3	2	1	0												
09-11									0	1	0	0	0	0	1	2	3	6	3	4	1	1	1	1	1	0						
11-13					0	1	0	0	2	0	1	0	2	0	1	2	2	2	1	3	2	2	4	2	1	2	0					
0040-42												0	1	1	8	6	2	4	1	0												
42-44															0	2	10	4	6	2	0	1										
44-46															0	6	3	2	0													
46-48															0	17	3	0	1													

APPENDIX I Sample Data of the Electric Charges on Precipitation